

Phase slips in submicrometer $\text{YBaCu}_3\text{O}_{7-\delta}$ bridges

P. Mikheenko, X. Deng, S. Gildert, M. S. Colclough, R. A. Smith, and C. M. Muirhead
School of Physics and Astronomy, University of Birmingham, Edgbaston, Birmingham B15 2TT, England

P. D. Prewett and J. Teng

School of Engineering, University of Birmingham, Edgbaston, Birmingham B15 2TT, England

(Received 3 August 2005; revised manuscript received 7 September 2005; published 7 November 2005)

We have measured the resistance vs temperature, $R(T)$, and current vs voltage, $I(V)$, for a series of submicrometer $\text{YBa}_2\text{Cu}_3\text{O}_{7-\delta}$ tracks. We find that superconductivity is suppressed when the room temperature resistance is greater than the superconducting resistance quantum, $R_q = h/4e^2$. In addition, we observe regular steps in the $I(V)$ characteristics of some bridges, which we associate with phase slip centers. For one bridge, with resistance just below the resistance quantum, R_q , we find a gradual entry into the superconducting state which is well fit by theoretical predictions for thermally activated phase slips in a superconducting wire.

DOI: [10.1103/PhysRevB.72.174506](https://doi.org/10.1103/PhysRevB.72.174506)

PACS number(s): 74.40.+k, 74.72.-h, 74.78.Na

I. INTRODUCTION

The mechanism by which superconductivity is suppressed in very narrow wires is of fundamental importance. Phase slips give rise to finite resistance in narrow superconducting wires below the transition temperature T_c . In a phase slip, the amplitude of the superconducting order parameter fluctuates to zero at some point along the wire, allowing the phase of the order parameter to slip by 2π . Such phase slips require activation across a free energy barrier, and this activation may occur either thermally or quantum mechanically. The theory of thermally activated phase slips (TAPS) was developed in the late 1960s by Langer, Ambegaokar, McCumber, and Halperin^{1,2} (LAMH). The resistance vs temperature takes the form

$$R_{\text{LAMH}}(T) = \left(\frac{h}{4e^2} \right) \left(\frac{\hbar\Omega}{k_B T} \right) e^{-\Delta F/k_B T}, \quad (1)$$

where $\Delta F = (8\sqrt{2}/3)(H_c^2/8\pi)A\xi$ is the energy barrier for phase slip nucleation, $\Omega = (L/\xi)(\Delta F/k_B T)(1/\tau_{\text{GL}})$ is the attempt frequency, $\tau_{\text{GL}} = [\pi\hbar/8k_B(T_c - T)]$ is the Ginzburg-Landau (GL) relaxation time, L is the length of the wire, A is its cross-sectional area, and ξ is the GL coherence length. Such behavior was subsequently observed in tin whiskers^{3,4} in the early 1970s.

Quantum phase slips (QPS) began to be considered theoretically and experimentally in the late 1980s. Saito and Murayama^{5,6} developed a theory of QPS which was a straightforward analog of the TAPS theory of LAMH. At about the same time, Giordano⁷⁻¹¹ observed $R(T)$ data in thin (40–100 nm diameter) In and PbIn wires which showed a crossover from LAMH behavior near T_c to a weak temperature dependence at a lower temperature. This was suggestive of QPS being dominant at low temperatures, although an alternative explanation for this behavior is granularity in the wires. Sharifi *et al.*¹² fabricated homogeneous Pb wires (15–95 nm wide, 1–10 nm thick) and found a systematic broadening of the $R(T)$ data away from the LAMH predictions as the cross-sectional area of the wires decreased. However, they found no evidence of QPS, i.e., no finite resistance

at low temperatures. Clear evidence of QPS was seen by Bezryadin *et al.*¹³ in ultrathin (5–10 nm diameter) nanowires of MoGe fabricated on carbon nanotubes. As the diameter of the wires decreased, the $R(T)$ data broadened, until a transition from superconducting to insulating behavior occurred. This was found to take place when the normal state resistance R_n increased above the superconducting resistance quantum, $R_q = h/4e^2 \approx 6.45$ k Ω . Later data on a larger sample of wires¹⁴ showed that behavior was determined by resistance per length, R_n/L , not resistance itself. Moreover, the data could be fitted by a model which included both^{14,15} QPS and TAPS. Such a model yields a smooth crossover from superconducting to insulating behavior, rather than a sharp transition. Since this work, several other nanowire systems have been experimentally investigated. Rogachev *et al.*¹⁶ studied the effect of high magnetic fields on $R(T)$ data of ~ 10 nm diameter Nb and MoGe wires. They found that their data could be explained by TAPS alone with a magnetic-field-dependent transition temperature, $T_c(B)$, and found no evidence of QPS. Kociak *et al.*¹⁷ made $R(T)$ measurements in ropes of single-wall carbon nanotubes and controversially claimed to see a superconducting transition. Their data has, however, recently been fitted to LAMH theory by Zhao,¹⁸ which gives some support to their interpretation. Phase slips and the flow of current in filaments has also previously been proposed to explain resistivity close to T_c in unpatterned $\text{YBa}_2\text{Cu}_3\text{O}_7$ (YBCO) films.^{19,20}

At currents above the critical current I_c , current-driven phase slip centers (PSCs) have also been observed in both low-temperature superconductors²¹ and high-temperature superconductors.^{22,23} These manifest themselves as a series of rather regular voltage steps in the $I(V)$ characteristics. Each step corresponds to the formation of an additional PSC and a corresponding increase in the differential resistance.

In this paper, we report preliminary measurements on five nanobridges of the high temperature superconductor YBCO. The data strongly suggest phase slip phenomena are occurring in our samples. As the room temperature resistance increases, we see a crossover from superconducting to insulating behavior—we find that bridges with $R_n < R_q$ show

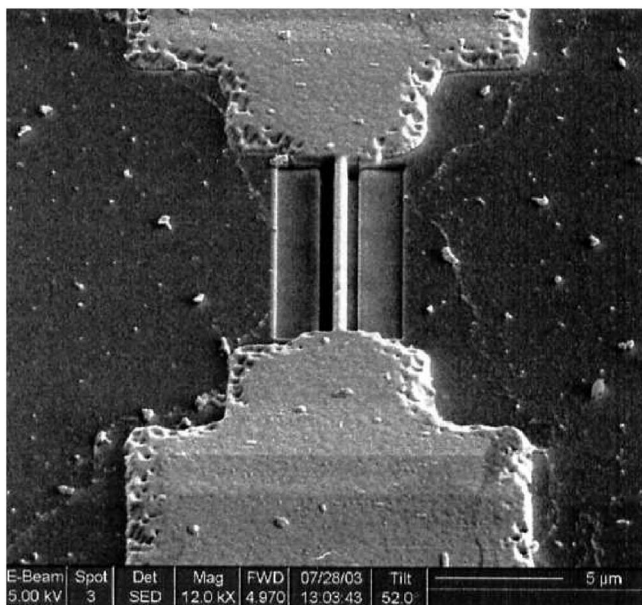


FIG. 1. Scanning electron microscope image of a submicrometer bridge produced by focused ion beam lithography. The central light region is the YBCO bridge. Two successive milling processes have reduced the bridge width to 500 nm.

superconductivity, while those with $R_n > R_q$ do not. The resistance vs temperature, $R(T)$, of the bridge with room temperature resistance closest to R_q shows the thermally activated phase slip form given in Eq. (1), a characteristic signature of phase slips. Very similar behavior has previously been seen in ultranarrow wires of the low- T_c superconductor¹³ MoGe. This suggests that we are observing both thermally activated and quantum phase slips in our submicrometer YBCO bridges, leading to a superconductor-insulator transition as their normal state resistance is increased above R_q . At currents above the critical current I_c , we also see steps in the $I(V)$ curves which are again characteristic²¹ of phase slip processes.

II. EXPERIMENTAL METHOD

YBCO films were deposited epitaxially onto (001) polished SrTiO₃ (STO) substrates using pulsed laser deposition. All films were 150 nm thick, apart from one which was 300 nm thick. Epitaxy and film quality were confirmed by x-ray diffraction (XRD) and the sharp 90 K transitions of the films prior to patterning into submicrometer bridges. Conventional optical lithography was used to produce bridges of width about 3 μm. These were then patterned by focused ion beam (FIB) lithography using a beam of gallium ions focussed down to 7 nm and raster scanned over a rectangular area to remove the YBCO. The beam current ranged from 100 to 500 pA, and the milling time was adjusted to ensure that there was clear penetration into the STO substrate, confirming that all the YBCO in the milled region was removed. By this means, we made a series of bridges between 5 and 10 μm long with widths ranging from 50 to 500 nm. In all, five bridges from four separate films were studied, including

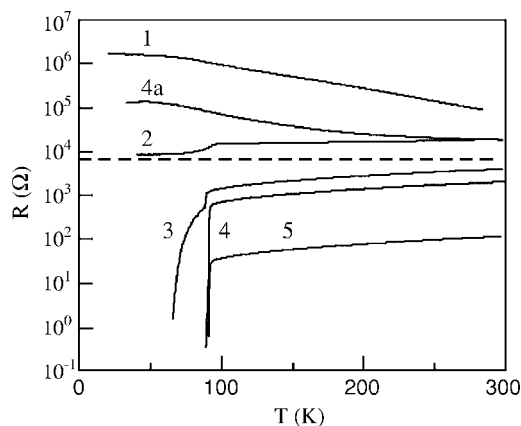


FIG. 2. Temperature dependence of the resistance of five YBCO bridges. The dashed line is the quantum of resistance $R_q = h/4e^2 \approx 6.45$ kΩ. The bridge widths are (1) 50 nm, (2) 100 nm, (3) 500 nm, (4) 100 nm, (5) 3 μm. Bridge 4a is bridge 4 after thermal cycling (see text). Bridges 1–4 have thickness 150 nm, while bridge 5 has thickness 300 nm.

a photolithographically patterned 3-μm-wide, 300-nm-thick bridge. A typical bridge is shown in Fig. 1. The milling was conducted in two stages: first the outer rectangles were removed, and then the beam current was reduced in order to trim the bridge width down to the required value. The bridge dimensions have been estimated from scanning electron microscopy (SEM) photographs. We note that the bridges are smooth on the scale of the Pearl penetration depth, so that formation of Abrikosov vortices will be suppressed.

Measurements of the resistance were made using a dc current and a four-point resistance method. We note, however, that for most samples, the resistance is dominated by the submicrometer bridge, rather than the much wider attached areas of YBCO film (which we refer to henceforth as contact pads). The resistance measurement is therefore effectively two point.

III. RESULTS AND INTERPRETATION

The resistance vs temperature, $R(T)$, characteristics for the five bridges are shown in Fig. 2. The measurement currents used were in the range 1–10 μA for bridges 1–4 and 30 μA for the widest, bridge 5. We saw no significant dependence on measuring current in this range. We note the following features:

(1) Bridge 5 is the unmilled bridge and reflects the combined resistance of the bridge and the remainder of the lithographically patterned film up to the voltage contacts. The value of 30 Ω is consistent with what we would expect from the resistivity of YBCO at 300 K and the geometry of the system. The resistances of the other samples above T_c , being at least a factor of 20 larger, must therefore be dominated by the resistance of the FIB fabricated bridges. The superconducting transition of the contact pads is normally unobservable on this larger resistance scale.

(2) There is a general tendency for the resistance to increase with decreasing bridge width, except that bridge 4 is

out of sequence. Bridge 4 is also anomalous in that, unlike the other bridges, which were stable with respect to thermal cycling, it degraded between two successive measurements. The later measurement is shown on the plot as 4a. The absence of a strictly monotonic change in behavior may represent experimental error in producing these structures, or defects in the YBCO film, which are quite likely on the submicrometer scale, and would not show up in XRD or T_c measurements. We should note that the diffusion of gallium ions into milled structures is a well-known problem with FIB and may well result in a degraded layer of YBCO at the surface, whose importance varies from sample to sample. An obvious consequence is that the relevant cross section of the bridges may be less than the measured values, a point we will return to later.

(3) The $R(T)$ characteristics can be divided into two quite distinct groups: (i) those which drop monotonically to a very low resistance at the lowest temperatures, and (ii) those which do not. The dotted line shows the superconducting quantum of resistance, $R_q = h/4e^2 = 6.45 \text{ k}\Omega$. We see that this lies more or less midway between the two groups. The transition to a quasi-insulating state above a resistance of order R_q is a well-known feature of low-dimensional superconductors. Whether the transition occurs at a universal value, and whether this value is exactly R_q , are highly contentious issues, both theoretically and experimentally. In superconductors, the coherence length is the characteristic length scale, and for YBCO this is around 0.25 nm in the crystallographic c direction and 1.5 nm in the ab plane for $T \ll T_c$. These are both much smaller than any of our sample dimensions, so low-dimensional behavior might not be initially expected. We, nevertheless, observe behavior in our samples characteristic of phase slip phenomena, and we explore this as an explanation of our results.

(4) The first strong piece of evidence for phase slip processes comes from the $I(V)$ characteristics below T_c , for which an example is shown in Fig. 3. We see successive steps that are associated with increased differential resistance as seen in other works and associated with^{21–23} PSCs. It has been proposed that such features may also be observed in two-dimensional superconductors where they result from the formation of phase slip lines²⁴ (PSLs). Whether our observed behavior is a result of PSCs or PSLs is unclear at this time, although the evidence from the $R(T)$ data below strongly favors the former interpretation.

(5) The second strong piece of evidence for phase slip processes comes from the $R(T)$ characteristic of the 500-nm-wide bridge 3. Here we see a sharp drop followed by a more gently falling resistance as T is lowered below T_c . This behavior is highly redolent of that observed in other work on low- T_c nanowires,^{13,14,16} where it has been strongly associated with phase slips. The sharp drop below T_c is interpreted as the superconducting transition of the two-dimensional YBCO contact pads; the smooth decrease is interpreted as the wider superconducting transition of the bridge and has the form associated with thermally activated phase slips predicted by LAMH and given in Eq. (1). We note that it is only the bridge whose room temperature resistance is closest to R_q which shows this behavior. The magnitude of the sharp drop below T_c may seem a little surprising, bearing in mind our

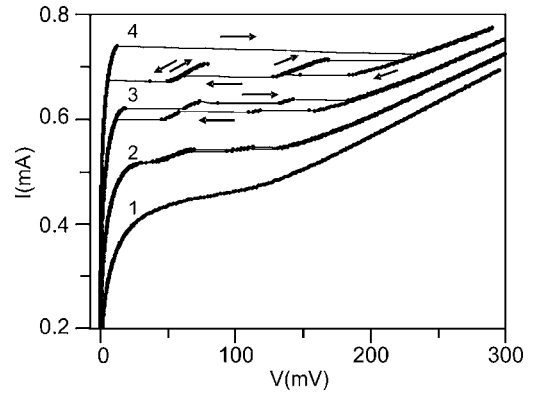


FIG. 3. Current-voltage characteristics of the 100 nm wide bridge 4 at temperatures: (1) 84.4 K, (2) 82.7 K, (3) 80.9 K, (4) 79 K. The voltage steps represent the nucleation of successive phase slip centers. Each step is associated with an increase in the differential resistance, as expected for an extra phase slip center, although these increments are not identical. Hysteresis at the highest temperature is negligible, but increases as the temperature is reduced. The approximately linear regions between the voltage steps are nonhysteretic, until the current is increased beyond some critical point, as shown for curve 4. Note that the negative slope of parts of the characteristics are due to the finite source resistance of our current supply.

estimate of 30Ω for the resistance of the contact pads. However the effective region of two-dimensional film may extend some distance into the submicrometer bridge and, hence, have a higher resistance than expected. We note that very similar behavior is seen in low- T_c bridges.¹³

(6) In order to carry out detailed fitting of the experimental $R(T)$ curve of bridge 3 to the LAMH prediction of Eq. (1), we need to make some assumptions about $H_c(T)$ and $\xi(T)$. In the absence of detailed experimental data for these quantities in YBCO, we have used the temperature dependences $H_c(T) = H_c(0)[1 - (T/T_c)]$ and $\xi(T) = \xi(0)[1 - T/T_c]^{-1/2}$. Taking into account the normal state resistance caused by electronic quasiparticles, which represents a parallel conduction channel, the total resistance from TAPS is

$$R = [R_N^{-1} + R_{\text{LAMH}}(T)]^{-1}. \quad (2)$$

Following Lau *et al.*¹⁴ and Rogachev *et al.*,¹⁶ we express the energy barrier as

$$\Delta F = 0.83(L/\xi_0)(R_q/R_n)k_B T_c (1 - T/T_c)^{3/2}. \quad (3)$$

In Fig. 4, we show a fit of Eq. (2) to our data for bridge 3, where we have used the measured values for L , R_n , and T_c . Considering that ξ_0 is our only variable parameter, the fit is quite good. However, this fit gives us a value for ξ_0 of $1.25 \mu\text{m}$, a factor of ~ 1000 greater than the accepted value, and a corresponding value for H_{c0} of 8 mT, which is a factor of ~ 2000 too small. Decoupling ξ_0 and H_{c0} , and using them as two separate variable parameters results in very little improvement to our fit and very little change to the fitting parameters. We cannot preclude the possibility that the track is, in some way, acting as though it had an effective coherence

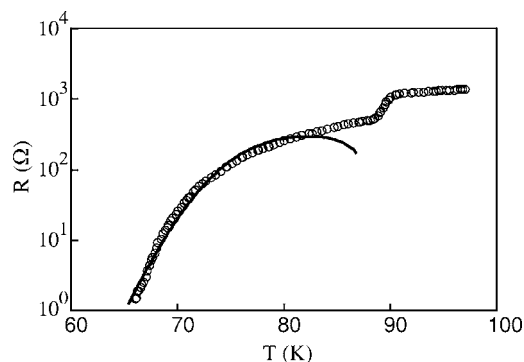


FIG. 4. Resistance vs temperature for the 500-nm-wide bridge 3. The open circles are the experimental data. The solid line is a fit to the LAMH theory for thermally activated phase slips as given in Eq. (2).

length of $1.25 \mu\text{m}$, and we note that this is at least consistent with the requirement that the effective value of ξ_0 is comparable with the sample dimensions, in order that phase slip processes can occur. This seems very unlikely, however, so we consider a more probable explanation. Using the same fit shown in Fig. 4, we now set ξ_0 to the realistic value of 1.5 nm , and the resistivity of YBCO at 90 K to $\rho = 3 \times 10^{-7} \Omega\text{m}$, and treat the cross-sectional area of the track (or, equivalently, the length) as our single variable parameter. We emphasize that this is not a new fit, simply a reinterpretation. We now find that $A = 4.7 \text{ nm}^2$, $L = 8.4 \text{ nm}$, and $H_{c0} = 2.56 \text{ T}$, the latter being about twice the published value of $H_{c0} = 1.4 \text{ T}$. Again, the cross section of the track is comparable in dimension with ξ_0 as required. The clear implication is that the thermally activated phase slippage is associated, not with the whole bridge, but with a dominant nanobridge having dimensions some three orders of magnitude smaller than the measured physical dimensions of the bridge. We have already noted that FIB milling results in Ga poisoning and that structural defects on the nanometer scale are quite likely. Either process could result in the nanobridge respon-

sible for the observed behavior. The unstable bridge 4 would then represent a sample in which the dominant nanobridge became degraded by thermal cycling and the value of R_n for this bridge (or another nanobridge) was above R_q .

(7) Finally it is clear that the fit to the data can only be worsened by the inclusion of quantum phase slip behavior, which has positive curvature and tends to a constant value at low temperatures. This has been confirmed by our attempts to fit to a combination of thermally activated and quantum phase slips (not shown). In any case, there is a clear need for a systematic study of the transition between the superconducting and resistive states in high-temperature superconductors in better controlled samples, in order that the development of thermally activated phase slips and the role of quantum phase slips can be clarified. Experiments are in hand to produce a single bridge whose normal state resistance can be controllably taken through R_q , with detailed measurements of $R(T)$ and $I(V)$ being made at each stage.

IV. CONCLUSIONS

We have reported the observation of a transition between the superconducting and resistive states in submicrometer high temperature superconductors bridges. We find that this transition occurs when the normal state resistance R_n passes through the resistance quantum, $R_q = h/4e^2$. For the bridge with R_n slightly below R_q , we observe a broadened transition which is well fit by the LAMH theory of TAPS with only a single fitting parameter. The active phase slip element appears to be a nanofilament of length $L \approx 8.4 \text{ nm}$ and cross-sectional area $A \approx 4.7 \text{ nm}^2$, which are much smaller than the physical dimensions of the bridge. This supports a picture of filamentary flow of current in high temperature superconductors. We also observe steps in the $I(V)$ characteristics at currents above the critical current I_c . These are typical of current-driven phase slip centers and provide further evidence that we are observing phase slip phenomena. We are currently working to produce samples suitable for more detailed and systematic investigation of these phenomena.

¹J. S. Langer and V. Ambegaokar, Phys. Rev. **164**, 498 (1967).

²D. E. McCumber and B. I. Halperin, Phys. Rev. B **1**, 1054 (1970).

³J. E. Lukens, R. J. Warburton, and W. W. Webb, Phys. Rev. Lett. **25**, 1180 (1970).

⁴R. S. Newbower, M. R. Beasley, and M. Tinkham, Phys. Rev. B **5**, 864 (1972).

⁵S. Saito and Y. Murayama, Phys. Lett. A **135**, 55 (1989).

⁶S. Saito and Y. Murayama, Phys. Lett. A **139**, 85 (1989).

⁷N. Giordano, Phys. Rev. Lett. **61**, 2137 (1988).

⁸N. Giordano and E. R. Schuler, Phys. Rev. Lett. **63**, 2417 (1989).

⁹N. Giordano, Phys. Rev. B **41**, 6350 (1990).

¹⁰N. Giordano, Phys. Rev. B **43**, 160 (1991).

¹¹N. Giordano, Physica B **203**, 460 (1994).

¹²F. Sharifi, A. V. Herzog, and R. C. Dynes, Phys. Rev. Lett. **71**, 428 (1993).

¹³A. Bezryadin, C. N. Lau, and M. Tinkham, Nature (London) **404**,

971 (2000).

¹⁴C. N. Lau, N. Marković, M. Bockrath, A. Bezryadin, and M. Tinkham, Phys. Rev. Lett. **87**, 217003 (2001).

¹⁵M. Tinkham, C. N. Lau, and N. Marković, Physica E (Amsterdam) **18**, 308 (2003).

¹⁶A. Rogachev, A. T. Bollinger, and A. Bezryadin, Phys. Rev. Lett. **94**, 017004 (2005).

¹⁷M. Kociak, A. Y. Kasumov, S. Guéron, B. Reulet, I. L. Khodos, Y. B. Gorbatov, V. T. Volkov, L. Vaccarini, and H. Bouchiat, Phys. Rev. Lett. **86**, 2416 (2001).

¹⁸G. M. Zhao, Phys. Rev. B **71**, 113404 (2005).

¹⁹M. M. Abdelhadi and J. A. Jung, Phys. Rev. B **67**, 054502 (2003).

²⁰J. Jung, M. Abdelhadi, H. Darhmaoui, and H. Yan, Int. J. Mod. Phys. B **19**, 167 (2005).

²¹W. J. Skocpol, M. R. Beasley, and M. Tinkham, J. Low Temp. Phys. **16**, 145 (1974).

- ²²F. S. Jelila, J.-P. Maneval, F. R. Ladan, F. Chibane, A. Marie-de-Ficquelmont, L. Méchin, J.-C. Villégier, M. Aprili, and J. Lesueur, Phys. Rev. Lett. **81**, 1933 (1998).
- ²³S. Reymond, L. Antognazza, M. Decroux, E. Koller, P. Reinert, and O. Fischer, Phys. Rev. B **66**, 014522 (2002).
- ²⁴A. G. Sivakov, A. M. Glukhov, A. N. Omelyanchouk, Y. Koval, P. Müller, and A. V. Ustinov, Phys. Rev. Lett. **91**, 267001 (2003).